

Meson Production In p-d Fusion To ${}^3\text{He}X$ At Proton Beam Momenta Between $p_p = 1.60 \text{ GeV}/c$ And $p_p = 1.74 \text{ GeV}/c$ With WASA-at-COSY

Nils Hüsken^{*†}

WWU Münster / WASA-at-COSY Collaboration

E-mail: n_hues02@uni-muenster.de

Florian Bergmann

WWU Münster / WASA-at-COSY Collaboration

E-mail: f_berg01@uni-muenster.de

Kay Demmich

WWU Münster / WASA-at-COSY Collaboration

E-mail: k.d@uni-muenster.de

Alfons Khoukaz

WWU Münster / WASA-at-COSY Collaboration

E-mail: khoukaz@uni-muenster.de

The production of (pseudoscalar) mesons in proton deuteron fusion to a ${}^3\text{He}$ nucleus and a mesonic system X has been a topic of active research for almost 30 years. Nonetheless, it still poses some open questions, most notably in the $pd (dp) \rightarrow {}^3\text{He}\eta$ and $pd (dp) \rightarrow {}^3\text{He}(\pi\pi)^0$ channels. The WASA-at-COSY Collaboration performed a new measurement in 2014 using the Wide Angle Shower Apparatus located inside the Cooler Synchrotron of the Forschungszentrum Jülich at 15 different beam momenta between $p_p = 1.60 \text{ GeV}/c$ and $p_p = 1.74 \text{ GeV}/c$ aiming to address some of these open questions. During the conference, recent preliminary results of the analysis of this new dataset were presented along with an outlook of the possibility this new dataset presents for the future.

The 26th International Nuclear Physics Conference

11-16 September, 2016

Adelaide, Australia

*Speaker.

†Supported by FFE program of the Forschungszentrum Jülich, the European Union Seventh Framework Programme (FP7/2007-2013) under grant agreement n 283286 and the Deutsche Forschungsgemeinschaft (DFG) through the Research Training Group GRK2149: "Strong and Weak Interactions - from Hadrons to Dark Matter".

1. Introduction

Ever since Bhalariao, Haider and Liu discovered the attractiveness of the ηN potential in 1985 [1][2], the production of η mesons off nuclei has received considerable experimental attention. Although the original calculations showed significant binding only for nuclei with $A \geq 12$, Wilkin among others later suggested the possible existence of η -nucleus bound states already for ${}^3\text{He}$ nuclei [3], inspiring a large search for such states in the $pd (dp) \rightarrow {}^3\text{He}\eta$ channel. As can be seen in Fig.1, the near threshold region has thus received considerable experimental attention, resulting in a large database up to an excess energy of about $Q \approx 10$ MeV [4] - [8].

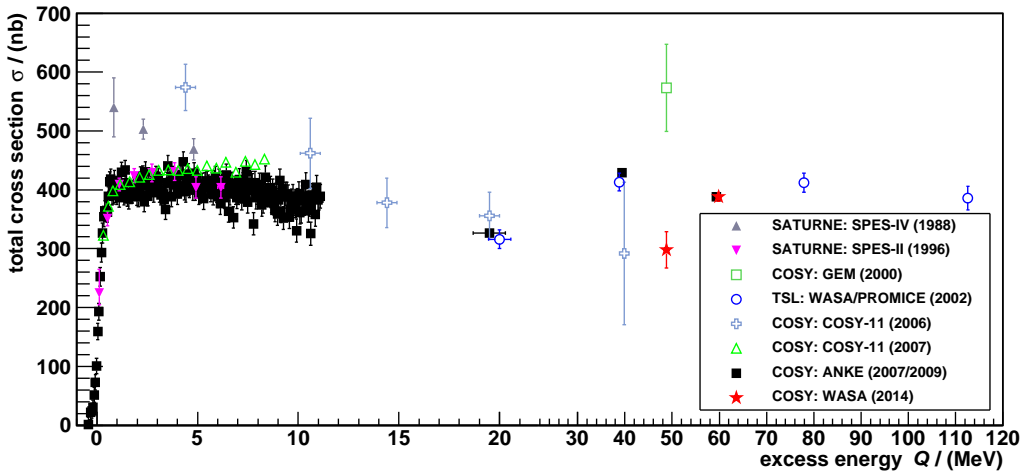


Figure 1: Total cross section data for the reaction $pd \rightarrow {}^3\text{He}\eta$ obtained by [4] - [13] as a function of the excess energy Q . Please note, that the scale was broken at $Q = 22$ MeV. Only statistical uncertainties are included. Figure taken from [13].

Away from threshold, however, the database becomes much more sparse with the available cross sections coming from [8] - [13]. Also, the different experiments and their associated systematics hinder a detailed study of the development of the differential cross sections with rising excess energy. Consequently, theoretical models trying to describe the ${}^3\text{He}\eta$ production at higher excess energies are much less refined than their near-threshold counterparts, where models based on optical potentials [14] as well as models based on two-step processes [15] both including a final state interaction, manage to describe the available data nicely. Therefore a recent review stated it would be *useful to obtain more data on this reaction at high energies in the future* [16]. For more details on η production, see the aforementioned review [16].

Alongside the production of η mesons, the production of single or multiple pions also warrants attention and is experimentally accessible within the new dataset presented during the conference. Single pion production in the reaction $pd (dp) \rightarrow {}^3\text{He}\pi^0$ has been extensively used as a normalization channel for measurements of the type $pd (dp) \rightarrow {}^3\text{He}X$ due its large available database [17][18] at scattering angles $\cos\vartheta_{\pi^0}^{cm} = \pm 1$ (the differential cross sections for $\cos\vartheta_{\pi^0}^{cm} = -1$ are displayed in Fig.2) along with the experimentally favorable feature of having the same final state particle in missing mass analyses.

In spite of this detailed knowledge of the cross sections in the case of very forward and very backward scattered pions, data on full differential cross sections or even parts of the angular range are rare. In fact, in the momentum range covered by the presented dataset, no additional information on differential cross sections can be found in the literature. A measurement of the angular distributions as far as covered by the WASA geometrical acceptance is therefore desirable.

The simultaneous production of two pions off ${}^3\text{He}$ nuclei received considerable attention ever since Abashian, Booth and Crowe discovered an unexpected enhancement for small $\pi\pi$ invariant masses in an inclusive $pd \rightarrow {}^3\text{He}X$ measurement [19], that was later confirmed in exclusive measurements [20]. Recently, a resonant structure was found in the basic double pionic fusion $pn \rightarrow d\pi^0\pi^0$ [21] (see Fig.3) at $m \approx 2.37$ GeV with a width of $\Gamma \approx 70$ MeV and subsequently confirmed in $pd \rightarrow {}^3\text{He}\pi^0\pi^0$ among other channels [22].

The dataset presented covers the near maximum region of the resonance in the $pd \rightarrow {}^3\text{He}(\pi\pi)^0$ case, so that the prospects of revisiting this channel with high statistics were explored.

2. The Experiment

The Wide Angle Shower Apparatus (WASA) is an internal fixed target experiment located at the Cooler Synchrotron (COSY) of the Forschungszentrum Jülich, Germany. It consists of two main detector parts (as visualized in Fig.4). The Central Detector, built around the interaction point where the beam particles interact with the frozen hydrogen or deuterium pellet target, utilizes the magnetic field of a solenoid to track charged particles stemming from meson decays in a drift chamber. A plastic scintillator and a calorimeter can be used for particle identification and energy measurements with the latter detector also being used for the detection of photons from neutral meson decays. Due to the fixed target geometry, a forward detection system is used for the detection of the heavier ejectiles like protons, deuterons and Helium nuclei. A proportional chamber allows the extraction of the polar and azimuthal angles of scattered particles, while various layers of scintillators are used for particle identification and energy reconstruction of forward scattered ejectiles. More detailed information on the WASA detector can be found in [23].

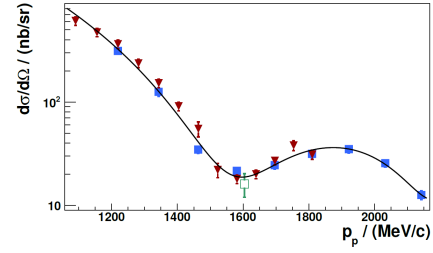


Figure 2: Differential cross section data at $\cos\vartheta_{\pi^0}^{cm} = -1$ for the reaction $pd \rightarrow {}^3\text{He}\pi^0$ from [17] (open squares) and [18] (triangles), as well as for the reaction $pd \rightarrow {}^3\text{H}\pi^+$ from [17] (filled squares, scaled by an isospin factor of 0.5) as a function of beam proton momentum. Figure adapted from [13].

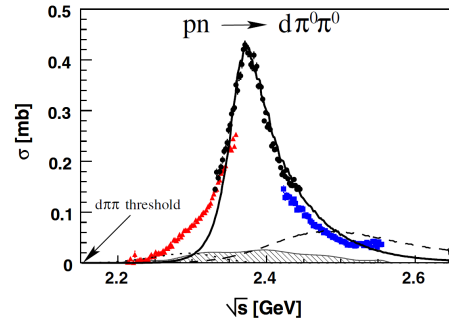


Figure 3: Total cross section for the reaction $pd \rightarrow d\pi^0\pi^0 p_{\text{spec}}$ as a function of center of mass energy, obtained by [21] for beam energies $T_p = 1.0$ GeV (triangles), $T_p = 1.2$ GeV (dots), and $T_p = 1.4$ GeV (squares). The hatched area represents systematic uncertainties, whereas the lines represent Roper excitation (dotted), t -channel $\Delta\Delta$ excitation (dashed) and excitation of the new resonance (solid). Figure taken from [21].

During the measurement presented at the conference, the so-called supercycle mode of the accelerator was taken advantage of, therefore minimizing the systematics between different beam momenta by alternating them between each new injection of a beam proton bunch. These beam protons with momenta in the range between $p_p = 1.60 \text{ GeV}/c$ and $p_p = 1.74 \text{ GeV}/c$ in steps of $p_{\text{step}} = 0.01 \text{ GeV}/c$ where then collided with a deuterium pellet target. Subsequently, Helium nuclei produced in these interactions were identified in the Forward Detector by their characteristically high energy loss (see Fig.5). As can be seen from Fig.6, the two-particle final states ${}^3\text{He}\eta$ and ${}^3\text{He}\pi^0$ can easily be identified in plots of the polar scattering angle of the Helium nuclei versus their reconstructed kinetic energy, making these plots a valuable tool in evaluating the quality of the detector calibration.

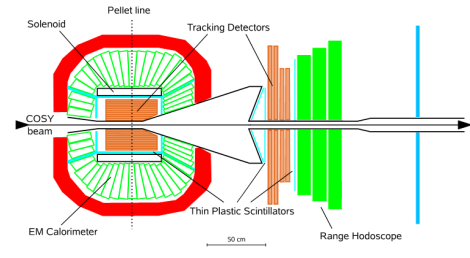


Figure 4: Schematic view of the WASA detector and its various detector parts. For more details, see text. Adapted from [23].

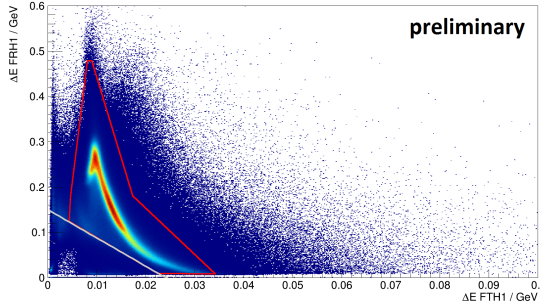


Figure 5: Energy loss in two different layers of the Forward Detector. The Helium band is clearly visible. The gray line represents a cut used for preselection, whereas the red line represents a cut as used in the analysis.

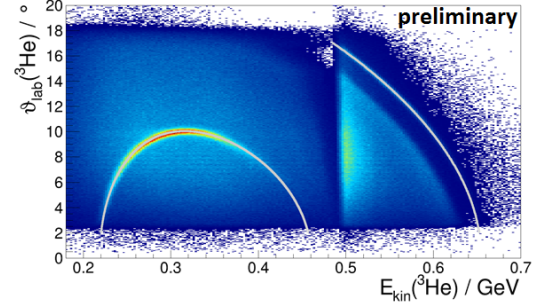


Figure 6: Distribution of the polar angle versus the reconstructed kinetic energy of identified Helium nuclei, which can be directly compared to kinematical relations for the two-particle final states ${}^3\text{He}\eta$ (left gray curve) and ${}^3\text{He}\pi^0$ (right gray curve).

3. η production

Due to four-momentum conservation, the η meson itself does not have to be reconstructed by its decay products, but it is in fact sufficient to use the absolute value of the momentum of the Helium nucleus in the center-of-mass system to identify the η production reaction (see Fig.7). These spectra of the final state momentum p are extracted in 25 bins of $\cos\vartheta_{\eta}^{cm}$. The background from multipion production channels can be subtracted using a fit based on Monte Carlo Simulations of two- and three-pion production with the fit excluding the peak region (as shown in Fig.7). In this way, angular distributions can be derived for all 15 beam momenta. The distribution for a beam momentum of $p_p = 1.70 \text{ GeV}/c$ can be seen in Fig.8. The angular distribution was normalized to match the total cross section value of $\sigma = 388.1 \text{ nb}$ measured by the ANKE experiment [9]. In order to investigate the systematics between distinct parts of the beam time, this momentum was measured in all three beam time periods.

Fig.8 illustrates that there is no visible systematic between the beam time periods, as all three angular distributions coincide. Also, a comparison to angular distributions derived in [9] and [13] can be done. As the data from [13] was also extracted with the WASA experiment, the apparent agreement comes at no surprise. The deviation between the angular distributions as measured with the WASA and ANKE experiments is a clear sign of the systematics between the different experiments involved and will need further investigation.

As the luminosity determination for the measurement presented is still a work in progress, no total cross sections were reported during the conference.

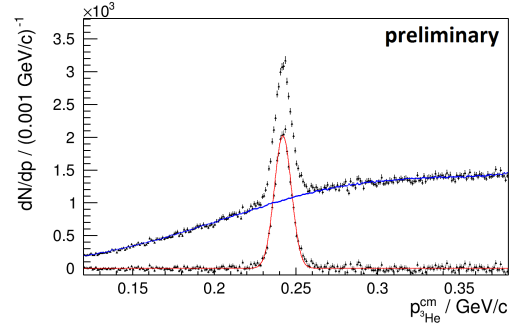


Figure 7: Final state momentum of reconstructed Helium nuclei in the center-of-mass system (black data). The background can be described by a fit (blue line) based on Monte Carlo simulations of two- and three-pion production. After subtraction (gray data), a gaussian signal is left (red line).

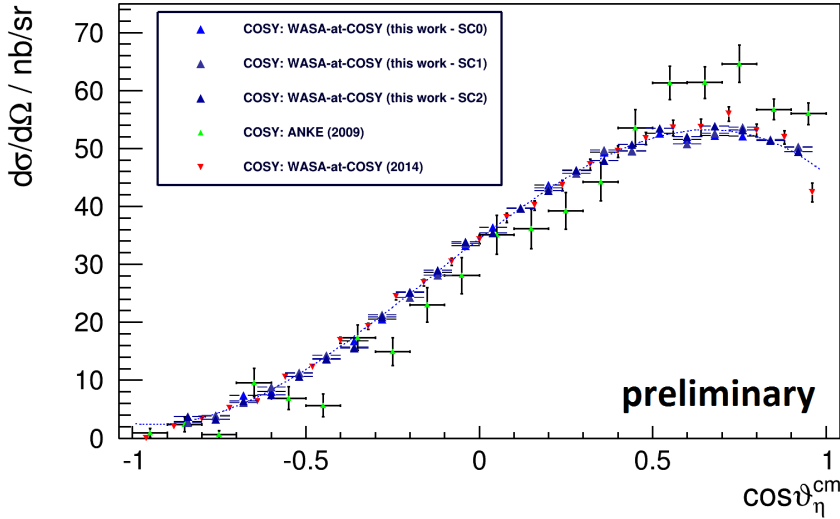


Figure 8: Angular distribution of the reaction $pd \rightarrow {}^3\text{He}\eta$ at $Q_\eta \approx 60$ MeV. Blue upward triangles represent the current work normalized to the total cross section value of $\sigma = 388.1$ nb measured by the ANKE experiment [9], which is shown as green upward triangles. Also shown are the data from [13] as red downward triangles.

4. π^0 production

Similar as in the η production case, the final state momentum of the Helium nucleus in the center-of-mass system can be used to quantify the ${}^3\text{He}\pi^0$ channel by means of fits to final state momentum spectra binned in $\cos\vartheta_{\pi^0}^{\text{cm}}$ (as shown in Fig.9). In this way, angular distributions are extracted for the part of backward scattered pions the WASA geometrical acceptance covers. The

non-normalized angular distributions extracted in this way for the 15 different beam momenta are displayed in Fig.10.

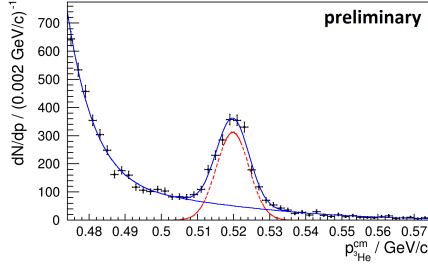


Figure 9: Final state momentum of reconstructed Helium nuclei in the center-of-mass system (black data). The spectrum can be described by an exponential plus polynomial background (blue line) as well as a gaussian signal (red line).

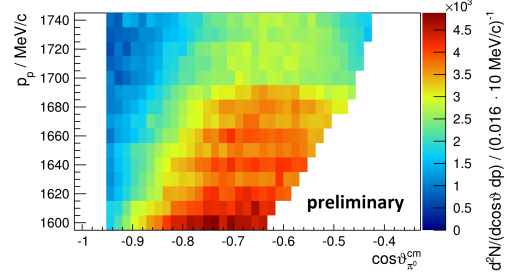


Figure 10: Angular distributions of the reaction $pd \rightarrow {}^3\text{He}\pi^0$ as a function of beam momentum p_p . The edges at the left and the right side of the histogram represent the geometrical acceptance of the WASA detector.

5. Multipion production

Lastly, a first exploration of the prospects of analyzing ${}^3\text{He}\pi^0\pi^0$ final states was presented [24]. The neutral pions in the Central Detector are reconstructed by their decay into two photons. Using only events with exactly two reconstructed π^0 mesons with an invariant mass matching the missing mass of the ${}^3\text{He}$ nucleus within the window displayed in Fig.11 (among other selection criteria discussed in [24]), clean samples of the ${}^3\text{He}\pi^0\pi^0$ final state can be extracted. Fig.12 shows the invariant mass of the two-pion system as well as for the ${}^3\text{He}\pi^0$ system for a beam momentum of $p_p = 1.60$ GeV/c after application of a kinematic fit and correcting for the acceptance. The enhancement over phase space distributions (shown as the gray shaded histograms) for small invariant masses of the $\pi^0\pi^0$ system can be observed along with an apparent peak in the ${}^3\text{He}\pi^0$ invariant mass, clearly hinting at the involvement of Δ resonances in the production process. With the statistics gathered in the presented measurement, the prospects of analyzing double-pion production in proton-deuteron fusion in high detail are excellent and further studies on both the invariant mass distributions as well as angular distributions and the dependence of said distributions on the beam momentum will be done in the future.

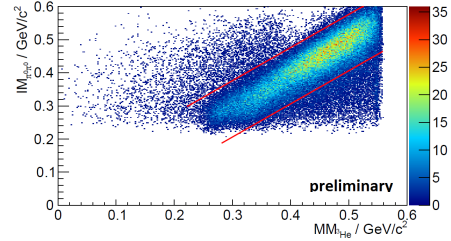


Figure 11: Invariant mass of the $\pi^0\pi^0$ system plotted against the missing mass of the corresponding Helium nucleus. The red lines represent the applied cut window [24].

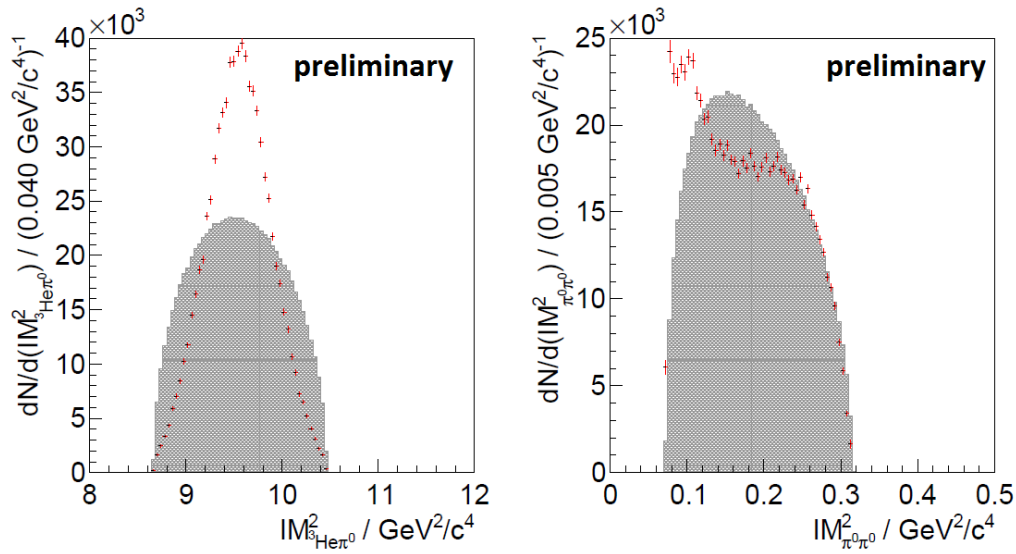


Figure 12: Invariant mass squared of the $\pi^0\pi^0$ system (left) and the ${}^3\text{He}\pi^0$ system (right). Red points correspond to data, gray shaded histograms show phase space distributions of the same integral [24].

6. Summary & Outlook

A new measurement of meson production in reactions of the type $pd \rightarrow {}^3\text{He}X$ was presented. Benefiting from the supercycle mode of the COSY accelerator, the systematics between the measurements at 15 different beam momenta in the range between $p_p = 1.60$ GeV/ c and $p_p = 1.74$ GeV/ c are minimal. Therefore, the prospects of studying the energy dependence of angular distributions of the single meson production reactions $pd \rightarrow {}^3\text{He}\eta$ and $pd \rightarrow {}^3\text{He}\pi^0$ were shown to be excellent. First angular distributions were shown with final differential cross sections being available soon.

In addition to single meson production, the prospects of analyzing the ABC effect in double-pion production were studied and first invariant mass distributions were presented during the conference. As it could be shown that the high statistics of the new dataset allows such studies in unprecedented detail, a more detailed investigation of double-pion production will soon be available.

References

- [1] R.S. Bhalerao *et al.*, *Off-shell model for threshold pionic η production on a nucleon and for ηN scattering*, *Phys. Rev. Lett.* **54**, 865 (1985).
- [2] Q. Haider *et al.*, *Formation of an eta-mesic nucleus*, *Phys. Lett. B* **172**, 257 (1986).
- [3] C. Wilkin, *Near-Threshold Production of η -Mesons*, *Phys. Rev. C* **47**, R938(R) (1993) [nucl-th/9301006v1].
- [4] T. Mersmann *et al.*, *Precision study of the $\eta - {}^3\text{He}$ system using the $dp \rightarrow {}^3\text{He}\eta$ reaction*, *Phys. Rev. Lett.* **98**, 242301 (2007) [nucl-ex/0701072v1].
- [5] J. Smyrski *et al.*, *Measurement of the $dp \rightarrow {}^3\text{He}\eta$ reaction near threshold*, *Phys. Lett. B* **649**, 258 (2007) [nucl-ex/0702043v1].

- [6] J. Berger *et al.*, Identification of the $dp \rightarrow {}^3\text{He}\eta$ Reaction Very Near Threshold: Cross Section and Deuteron Tensor Analyzing Power, *Phys. Rev. Lett.* **61**, 919 (1988).
- [7] B. Mayer *et al.*, Reactions $pd \rightarrow {}^3\text{He}\eta$ and $pd \rightarrow {}^3\text{He}\pi^+\pi^-$ near the η threshold, *Phys. Rev. C* **53**, 2068 (1996).
- [8] H.-H. Adam *et al.*, Hadronic ${}^3\text{He}\eta$ production near threshold, *Phys. Rev. C* **75**, 014004 (2007).
- [9] T. Rausmann *et al.*, Precision study of the $dp \rightarrow {}^3\text{He}\eta$ reaction for excess energies between 20 and 60 MeV, *Phys. Rev. C* **80**, 017001 (2009) [0905.4595v1 [nucl-ex]].
- [10] R. Bilger *et al.*, Measurement of the $\vec{p}d \rightarrow {}^3\text{He}\eta$ cross section between 930 and 1100 MeV, *Phys. Rev. C* **65**, 044608 (2002).
- [11] R. Bilger *et al.*, Measurement of the $pd \rightarrow pd\eta$ cross section in complete kinematics, *Phys. Rev. C* **69**, 014003 (2004).
- [12] M. Betigeri *et al.*, Measurement of $p+d \rightarrow {}^3\text{He} + \eta$ in S_{11} Resonance, *Phys. Lett. B* **472**, 267 (2000) [nucl-ex/9912006].
- [13] P. Adlarson *et al.*, Cross section ratio and angular distributions of the reaction $p+d \rightarrow {}^3\text{He} + \eta$ at 48.8 MeV and 59.8 MeV excess energy, *Eur. Phys. J. A* **50**, 100 (2014) [1402.3469v2 [nucl-ex]].
- [14] J.-J. Xie *et al.*, Determination of the η - ${}^3\text{He}$ threshold structure from the low energy $pd \rightarrow \eta$ - ${}^3\text{He}$ reaction (2016), 1609.03399 [nucl-th].
- [15] K.P. Khemchandani *et al.*, Comment on "Hadronic ${}^3\text{He}\eta$ production near threshold", *Phys. Rev. C* **76**, 069801 (2007) [0712.1993v1 [nucl-th]].
- [16] N.G. Kelkar *et al.*, Interaction of eta mesons with nuclei, *Rep. Prog. Phys.* **76**, 066301 (2013) [1306.2909v2 [nucl-th]].
- [17] P. Berthet *et al.*, Very backward π^0 and η^0 production by proton projectiles on a deuterium target at intermediate energies, *Nucl. Phys. A* **443**, 589 (1985).
- [18] C. Kerboul *et al.*, Deuteron tensor analyzing power for the collinear $\vec{p}d \rightarrow {}^3\text{He}\pi^0$ reaction at intermediate energies, *Phys. Lett. B* **181**, 28 (1986).
- [19] N.E. Booth *et al.*, Possible Anomaly in Meson Production in $p+d$ Collisions, *Phys. Rev. Lett.* **5**: 258-260, (1960).
- [20] M. Bashkanov *et al.*, Exclusive Measurements of $pd \rightarrow {}^3\text{He}\pi\pi$: the ABC Effect Revisited, *Phys. Lett. B* **637**: 223-228, (2006) [nucl-ex/0508011v3].
- [21] P. Adlarson *et al.*, ABC Effect in Basic Double-Pionic Fusion — Observation of a new resonance?, *Phys. Rev. Lett.* **106**: 242302, (2011) [1104.0123v1 [nucl-ex]].
- [22] P. Adlarson *et al.*, ABC Effect and Resonance Structure in the Double-Pionic Fusion to ${}^3\text{He}$, *Phys. Rev. C* **91**, 015201, (2015) [1408.5744v1 [nucl-ex]].
- [23] H.-H. Adam *et al.*, Proposal for the Wide Angle Shower Apparatus (WASA) at COSY-Jülich "WASA-at-COSY", (2004), nucl-ex/0411038v1.
- [24] L. Wölfer, Studies on the Two-Pion Production in the Reaction $p+d \rightarrow {}^3\text{He} + X$ with Particular Regard to the ABC Effect, BSc Thesis, University of Münster, Germany, (2015).